

# Effect of ethylene oxide unit number in bis-EMA on the physical properties of additive-manufactured occlusal splint material

Junichiro Wada <sup>a,b,\*</sup>, Paulina Heponiemi <sup>a</sup>, Kanae Wada <sup>a,c</sup>, Sufyan Garoushi <sup>a</sup>,  
Noriyuki Wakabayashi <sup>b</sup>, Tsutomu Iwamoto <sup>c</sup>, Pekka K. Vallittu <sup>a,d</sup>, Lippo Lassila <sup>a</sup>

<sup>a</sup> Department of Biomaterials Science, Turku Clinical Biomaterials Centre - TCBC, Institute of Dentistry, University of Turku, Turku, Finland, <sup>b</sup> Department of Advanced Prosthodontics, Tokyo Medical and Dental University (TMDU), Tokyo, Japan, <sup>c</sup> Department of Pediatric Dentistry/Special Needs Dentistry, Tokyo Medical and Dental University (TMDU), Tokyo, Japan, <sup>d</sup> Wellbeing Services County of South-West Finland, Turku, Finland

## Abstract

**Purpose:** To investigate the effects of the number of ethylene oxide units in bis-EMA on the physical properties of additively manufactured occlusal splints.

**Methods:** Seven experimental materials containing bis-EMAs with three and 10 ethylene oxide units (BE3 and BE10, respectively) were prepared at different BE10 content rates (BE10-0%, -20%, -30%, -40%, -50%, -60%, and -80%). Half the specimens of each material were aged in boiling water. Flexural strength (FS), flexural modulus (FM), fracture toughness (FT), microwear depth (MD), degree of conversion (DC), water sorption (WSP), water solubility (WSL), color difference between non-aged and aged series ( $\Delta E$ ), and translucency (TP) were evaluated. All the evaluated properties other than FS and MD were analyzed by 1-way ANOVA and Tukey's post hoc analysis, while FS and MD were analyzed by Kruskal–Wallis's test and Bonferroni correction ( $\alpha=0.05$ ).

**Results:** BE10-80% revealed the lowest FS ( $P < 0.01$  for BE10-0%, -20%, and -30%) and FM ( $P < 0.01$ , for all), while revealing the highest DC, WSP, WSL ( $P < 0.01$  for all) and TP ( $P < 0.01$  for all other than BE10-60%). BE10-50% showed the highest FT ( $P < 0.01$  for all). BE10-50%, -60%, and -80% revealed significantly lower  $\Delta E$  than others ( $P < 0.01$ ) and lower MD than BE10-0% ( $P < 0.05$ ). Regardless of the BE10 content, FS, FM, and FT decreased with aging.

**Conclusions:** The number of ethylene oxide units affects the physical properties of additively manufactured occlusal splints. The higher number of ethylene oxide units in bis-EMA enhanced the microwear resistance, DC, WSP, WSL, color stability, and translucency, whereas it deteriorated the FS and FM.

**Keywords:** Additive manufacturing, Bis-EMA, Ethylene oxide unit, Occlusal splint, Physical property

Received 11 August 2023, Accepted 27 December 2023, Available online 29 January 2024

## 1. Introduction

Recently, the application of digital technology has rapidly spread in various dental fields. Owing to these digital manufacturing technologies, additive manufacturing (called “three-dimensional (3D) printing”) offers several advantages such as minimal material waste and low cost[1]. However, it results in objects with lower strength and fitting accuracy compared to subtractive manufacturing (called “milling”)[2,3]. Occlusal splints are oral appliances widely used for various purposes, including managing temporomandibular disorders[4–6], preventing tooth wear and fracture of fixed prostheses, especially those made of ceramic, due to severe sleep bruxism[7,8], and protecting mobile teeth weakened with severe periodontitis[9,10]. Furthermore, additive manufacturing has become more prevalent than subtractive manufacturing in digitally fabricating

occlusal splints. However, additively manufactured occlusal splints have shown inferior mechanical properties compared to their conventional counterparts[11].

According to previous reports, hard-type occlusal splints fabricated using heat-cured or auto-polymerizing poly (methyl methacrylate) (PMMA) are clinically preferred over soft splints fabricated using

### WHAT IS ALREADY KNOWN ABOUT THE TOPIC?

» Additive manufacturing (3D printing) is widely used for fabricating occlusal splints. Additive manufacturing offers several advantages, such as minimal material waste and low cost. However, compared to conventional occlusal splints, additive-manufactured occlusal splints exhibit inferior mechanical properties.

### WHAT THIS STUDY ADDS?

» Our study highlights that bis-EMA photosensitive monomers impact the physical properties of the materials used for additive-manufacturing occlusal splints. Higher numbers of ethylene oxide units in bis-EMA enhance the microwear resistance, degree of conversion, color stability during aging, and translucency of the materials.

DOI: [https://doi.org/10.2186/jpr.JPR\\_D\\_23\\_00203](https://doi.org/10.2186/jpr.JPR_D_23_00203)

\*Corresponding author: Junichiro Wada, Advanced Prosthodontics, Graduate School, Tokyo Medical and Dental University (TMDU), 1-5-45 Yushima, Bunkyo-ku, Tokyo 113-8549, Japan.

E-mail address: [wadajun.rpro@tmd.ac.jp](mailto:wadajun.rpro@tmd.ac.jp)

vacuum-formed thermoplastic materials such as polypropylene and polyethylene[12–15]. Conversely, a few reports have revealed some clinical benefits of soft occlusal splints such as effectiveness in treating myogenous temporomandibular disorders[16] and enhanced comfort for occlusal splint wearers[17]. In additive manufacturing, photosensitive materials are polymerized using light from the luminous source of a 3D printer. Bisphenol A-glycidyl methacrylate (bis-GMA) is commonly and traditionally used in dentistry as a photosensitive monomer of PMMA. However, Bis-GMA has a risk of incomplete polymerization with additive manufacturing owing to its high molecular weight and viscosity[18]. Ethoxylated bisphenol A dimethacrylate (bis-EMA) is also a photosensitive monomer of PMMA that shows high polymerization reactivity and biocompatibility[19]. Bis-EMA contains two aromatic groups that increase structural strength with three-dimensional networks, whereas it also contains ethylene oxide units that promote the growth of two-dimensional polymer chains. The hardness of the photosensitive PMMA and other physical properties depends on the content ratio of bis-EMA with varying numbers of ethylene oxide units.

Although the physical properties of conventional PMMA-based materials used for occlusal splints are generally sufficient for clinical use[20], the application of bis-EMA as a photosensitive monomer can deteriorate their physical properties. Additionally, degradation during clinical use is a critical factor that influences the physical properties of occlusal splints. Meanwhile, hydrolysis can degrade the physical properties of the occlusal splints used in the mouth.

Therefore, this study aimed to investigate the effects of bis-EMA content (with different numbers of ethylene oxide units) and aging in boiling water on the physical properties of experimentally fabricated materials used for additive-manufactured occlusal splints. The evaluated physical properties included flexural strength, flexural modulus, fracture toughness, microwear depth, degree of double-bond conversion, water sorption, water solubility, and color parameters. The tested null hypotheses are as follows: 1) the content rate of bis-EMA with different numbers of ethylene oxide units does not impact on the evaluated properties of additive-manufactured occlusal splint material and 2) aging in boiling water has no impact.

## 2. Materials and Methods

### 2.1. Specimen fabrication

The chemical structures and components of the experimental PMMA-based acrylic resins for the additive-manufactured occlusal splints tested in this study are shown in **Figure 1** and **Table 1**. Bis-EMA with three ethylene oxide units (BE3), bis-EMA with 10 ethylene oxide units (BE10), and urethane-dimethacrylate (UDMA) were mixed at weight ratios of 80 wt. % BE3+BE10 and 20 wt. % UDMA. Subsequently, trimethylbenzoyl diphenylphosphine oxide (TPO) was added at a concentration of 2 wt. %. Based on the weight ratios of BE3 to BE10, the prepared resins were classified into seven groups as listed in **Table 2**.

For each prepared resin, two sets of 16 bar-shaped specimens, with dimensions of 3.0 mm × 10.0 mm × 60.0 mm and 4.0 mm × 8.0 mm × 40.0 mm, were additive-manufactured by a digital light processing (DLP) printer with a light-emitting diode (LED) wavelength of 385 nm (Asiga MAX™, SCHEU-DENTAL GmbH, Iserlohn, Germany) for 3-point bending and fracture toughness tests, respectively. The size and number of specimens were standardized according to pre-

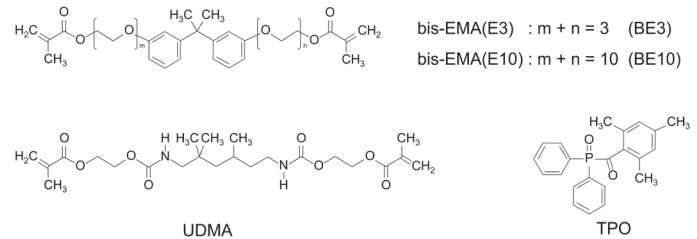


**Fig. 1.** Chemical structures of the monomers (bis-EMA[E3], bis-EMA[E10], and urethane-dimethacrylate [UDMA]) and initiator (trimethylbenzoyl diphenylphosphine oxide [TPO])

**Table 1.** Component materials of tested methacrylate-based acrylic resins for additive-manufactured occlusal splints

Component material	Molecular weight	Batch number	Manufacturer	Abbreviation
bis-EMA (E3) (Ethoxylated bisphenol A dimethacrylate with 3 ethylene oxide units)	496	811-51	ESSCHEM Europe Ltd, England	BE3
bis-EMA (E10) (Ethoxylated bisphenol A dimethacrylate with 10 ethylene oxide units)	804	815-325	ESSCHEM Europe Ltd, England	BE10
UDMA (Urethane acrylate methacrylate resin)	470	815-118	ESSCHEM Europe Ltd, England	-
TPO (Diphenyl(2,4,6-trimethylbenzoyl) phosphine oxide)	348	1376022	Abcr GmbH, Germany	-

**Table 2.** Compound weight ratios (wt %) of tested groups

Tested group	BE3	BE10	UDMA	TPO <sup>#</sup>
BE10-0%	80	0	20	2
BE10-20%	60	20	20	2
BE10-30%	50	30	20	2
BE10-40%	40	40	20	2
BE10-50%	30	50	20	2
BE10-60%	20	60	20	2
BE10-80%	0	80	20	2

<sup>#</sup>: TPO was added after mixture of BE3, BE10, and UDMA. UDMA: urethane-dimethacrylate, TPO: trimethylbenzoyl diphenylphosphine oxide.

vious studies[21,22]. Each additive manufacturing was performed in a horizontal direction with a layer thickness of 100 μm (**Fig. 2**). The additive-manufactured specimens were washed using 99% isopropanol for 10 min in an ultrasonic cleaning unit (Quantrex® 90, L&R Ultrasonics, New Jersey, USA) to remove the unpolymerized material, followed by stroboscopic post-curing on both sides using 2000 flashes with frequency, wavelength, and pressure of 10 Hz, 300–700 nm, and 120 KPa, respectively (Otoflash G171, BEGO GmbH & Co, Bremen, Germany) in the air atmosphere. Additionally, for each group, half of the post-cured specimens ( $n = 8$ ) were kept in distilled water for 72 h, followed by aging for 16 h at 100°C (aged series)[23,24]. However, the physical properties of the other half ( $n = 8$ ) were directly tested without any water storage or aging at 100°C (non-aged series). All tests except for the water solubility and sorption tests were performed at 23 ± 1°C and 40% humidity.

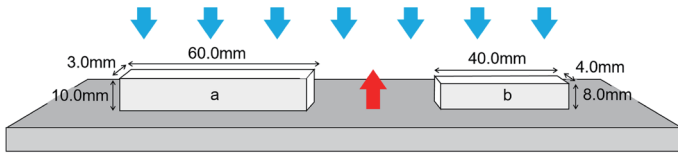


**Fig. 2.** Schematic illustration of the printing unit, where a and b are the specimens for the three-point bending and fracture toughness tests, respectively. Red arrows show the printing orientation, while blue arrows show the direction of light illumination.

## 2.2. Flexural strength and modulus

To assess the flexural strength and modulus, a three-point bending test was performed for both the non-aged and aged series of each tested resin using a universal testing machine (Model LRX; Lloyds Instruments Ltd., Hampshire, UK) in the air atmosphere at  $23 \pm 1^\circ\text{C}$  and 40% humidity, according to the ISO 20795-1 standard method[25]. A load cell with a capacity of 2500 N was used at a cross-head speed of 5.0 mm/min. The distance between the supports of the tested specimens was 50.0 mm. The endpoint of each test was specimen breaking. Alternatively, it was considered to be finished when the specimen deflection reached 8.0 mm or when the load reduction reached 10% of the maximum load. Flexural strength ( $\sigma$ ) was calculated in MPa using the following equation:

$$\sigma = \frac{3FL}{2b \times h^2},$$

where F is the maximum load applied to the specimen (N), L is the span length (50 mm), and b and h are the width (10 mm) and height (3 mm) of the specimen, respectively. The flexural modulus (E) was calculated in MPa using the following equation:

$$E = \frac{F}{d} \times \frac{L^3}{4b \times h^3},$$

where F/d is the gradient of the load–deflection curve in the linear section, L is the span length (50 mm), and b and h are the width (10 mm) and height (3 mm) of the specimen, respectively. In this study, the flexural modulus was converted from MPa to GPa. Additionally, the ratio of broken specimens to total specimens (%) and deflection at specimen break (mm) were recorded.

## 2.3. Fracture toughness

According to the ISO standard method[25], a single-edge notched bend (SENB) test was conducted to assess the fracture toughness of both the non-aged and aged series. A notch with a depth of 3.0 mm was made at the center of each specimen using a double-sided diamond disk with 0.15 mm thickness (Komet, Brassler, Legmo, Germany). Subsequently, the specimen was polished and sharpened using a straight-edged razor blade. The notch depth of each specimen was standardized using a light microscope (Leica Microsystems GmbH, Wetzlar, Germany). A three-point bending test was performed for each notched specimen using a universal testing machine with a crosshead speed and support distance of 1.0 mm/min and 32.0 mm, respectively. After the specimen fractured, the notch length on the fracture surface was measured three times using

a light microscope, and the mean value of the three measurements was defined as the crack length (mm). The fracture toughness was calculated in  $\text{MPa}\cdot\text{m}^{1/2}$  using the following equations:

$$K_{IC} = f(x) \cdot \left[ \frac{P \cdot L}{B \cdot W^2} \right] \cdot \sqrt{10^{-3}}$$

$$f(x) = 3 \sqrt{\frac{a}{W}} \cdot \frac{\left\{ 1.99 - \frac{a}{W} \cdot (1 - a/W) \cdot \left[ 2.15 - 3.93 \cdot a/W + 2.7 \cdot (a/W)^2 \right] \right\}}{\left\{ 2 \cdot (1 + a/W) \cdot (1 - a/W)^2 \right\}}$$

where  $K_{IC}$  is the fracture toughness ( $\text{MPa}\cdot\text{m}^{1/2}$ ), P is the maximum load (N), L is the span distance (mm), B is the specimen width (mm), W is the specimen thickness (mm), and a is the crack length (mm).

Additionally, the ratio of broken specimens to total specimens (%) and deflection at specimen break (mm) were recorded.

## 2.4. Microwear resistance (microwear depth)

For microwear evaluation, six specimens were randomly selected from each group of the non-aged specimens. Based on previous studies[11,26,27], a two-body wear test was performed to demonstrate the microwear resistance of each specimen. All selected specimens were sectioned (3.0 mm  $\times$  10.0 mm  $\times$  15.0 mm) and stored in water at  $37.0^\circ\text{C}$  for 24 h before testing. The microwear test was performed in a chewing simulator (CS-4.2, SD Mechatronik, Feldkirchen-Westerham, Germany), where two different chambers sequentially simulated vertical and horizontal movements in the presence of water. Each chamber included a lower sample holder to secure the specimen and an upper loading tip (a steatite ball with a diameter of 6 mm), serving as the antagonist. For each specimen, 15000 chewing cycles were performed at 1.5 Hz with a vertical weight of 2 kg, assuming a chewing force of 20 N. Wear patterns were scanned using a 3D optical profilometer (ContourGT-I, Bruker Nano, Inc., Tucson, AZ, USA), and the average of the deepest points of six profiles scanned in each specimen was calculated as the microwear depth ( $\mu\text{m}$ ), which is the representative value of microwear resistance.

## 2.5. Degree of double bond conversion (DC)

For the non-aged series, the degree of double bond conversion (DC) was evaluated for five specimens randomly selected after fracture toughness evaluation ( $n = 5/\text{subgroup}$ ). The DC was measured using a Fourier transform infrared (FT-IR) spectrometer (Frontier FT-IR spectrometer; PerkinElmer, Llantrisant, UK)[28]. The ratio of the intensity of the C-C double bond (aliphatic) absorbance peak at  $1638 \text{ cm}^{-1}$  was detected based on the aromatic reference peak at  $1600 \text{ cm}^{-1}$ . As a control, the ratio of the unpolymerized resin was determined in the same manner. The DC was calculated as a percentage using the following equation:

$$DC = 100 \cdot \left( 1 - \frac{C_{ali}/C_{aro}}{U_{ali}/U_{aro}} \right),$$

where  $C_{ali}$  is the ratio of aliphatic peaks in the polymerized specimen,  $C_{aro}$  is the ratio of aromatic peaks in the polymerized specimen,  $U_{ali}$  is the ratio of aliphatic peaks in the unpolymerized resin, and  $U_{aro}$  is the ratio of aromatic peaks in the unpolymerized resin.

## 2.6. Water sorption (WSP) and solubility (WSL)

The specimens of the non-aged series were sectioned (3.0 mm × 10.0 mm × 15.0 mm) after flexural strength and modulus testing to assess the water sorption ( $W_{SP}$ ) and solubility ( $W_{SL}$ ) ( $n = 8$ /subgroup). As the first drying procedure, each specimen was dried in a vacuum desiccator containing freshly dried silica at  $37 \pm 1$  °C for 22 h and then at  $23 \pm 1$  °C for 2 h. The initial weight ( $WT_1$ ) of each specimen was measured using a digital analytical balance (XS105; Mettler Toledo, Greifensee, Switzerland) with an accuracy of 0.1 mg. Then, the first drying procedure was continued until the weight decrease was less than 0.1 mg for all the specimens. After the stabilization of the weights of all specimens, the specimens were immersed in 50.0 mL of distilled water and stored at 37 °C for 30 days (the water immersion procedure). The weights of the water-immersed specimens were measured 60 s after removal from water, and the specimens were carefully dried with absorbent paper at 1, 2, 3, 7, 14, 21, 28, and 30 d after immersion in water (the weight at 30 d was named  $WT_2$ ). Finally, in the same manner as the first drying procedure, the second drying procedure was continued until a stable weight ( $WT_3$ ) was achieved for each specimen.  $W_{SP}$  and  $W_{SL}$  were calculated (%) using the following equations:

$$W_{SP} = 100 \cdot \frac{WT_2 - WT_3}{WT_1},$$

$$W_{SL} = 100 \cdot \frac{WT_1 - WT_3}{WT_1},$$

where  $WT_1$  is the initial weight of the specimen after storage in a desiccator for 24 h (mg),  $WT_2$  is the weight of the specimen after water immersion for 30 d (mg), and  $WT_3$  is the stable weight of the specimen after the second drying cycle (mg).

## 2.7. Color evaluation (Spectrophotometric analysis)

After the fracture toughness evaluation, a spectrophotometric analysis was performed to assess the color of both the non-aged and aged subgroups. Before the evaluations, both surfaces of five specimens, randomly selected from each subgroup, were polished via wet polishing using a silicon carbide grinding paper 4000-grit with a grain size of 5 μm (SiC Paper #4000, Struers LLC, Cleveland, USA). According to the Commission International de l'Éclairage  $L^*a^*b^*$  (CIE Lab) color space system [29], the following three parameters were used for color evaluation: lightness/darkness as the  $L^*$  value (0 to 100 for black to white), greenness/redness as the  $a^*$  value (negative to positive values for green to red), and blueness/yellowness as the  $b^*$  value (negative to positive values for blue to yellow). A noncontact dental spectrophotometer (Crystaleye; Olympus, Tokyo, Japan) was calibrated according to the manufacturer's instructions before each measurement. The  $L^*$ ,  $a^*$ , and  $b^*$  values of the polished surfaces of each specimen were evaluated ( $n = 5$ /subgroup). For each content rate of BE10, the color difference between non-aged and aged subgroups ( $\Delta E$ ) was calculated as the color stability during aging by the following equations:

$$\Delta E = \sqrt{(L_N^* - L_A^*)^2 + (a_N^* - a_A^*)^2 + (b_N^* - b_A^*)^2},$$

where  $L_N^*$ ,  $a_N^*$ , and  $b_N^*$  are the mean  $L^*$ ,  $a^*$ , and  $b^*$  values of the non-aged specimens, respectively, and  $L_A^*$ ,  $a_A^*$ , and  $b_A^*$  are the mean  $L^*$ ,  $a^*$ , and  $b^*$  values of the aged specimens, respectively.

Additionally, for both the non-aged and aged series, the translucency parameter (TP) of each specimen was calculated using the following equation:

$$TP = \sqrt{(L_W^* - L_B^*)^2 + (a_W^* - a_B^*)^2 + (b_W^* - b_B^*)^2},$$

where  $L_W^*$ ,  $a_W^*$ , and  $b_W^*$  are the  $L^*$ ,  $a^*$ , and  $b^*$  values, respectively, when the specimens were evaluated on a white background, and  $L_B^*$ ,  $a_B^*$ , and  $b_B^*$  are the  $L^*$ ,  $a^*$ , and  $b^*$ , respectively, when the specimens were evaluated on a black background.

## 2.8. Statistical analysis

For all the acquired data, except the flexural strength, specimen deflection during the three-point bending tests, and microwear depth, the equality and normality were validated by the Levene and Shapiro–Wilk tests, respectively. A two-way analysis of variance (ANOVA) was performed to detect the effects of the content rate of BE10 and aging in boiling water (as independent variables) on the flexural modulus, fracture toughness,  $\Delta E$ , and TP. Additionally, using a one-way ANOVA followed by a Tukey multiple comparison post hoc analysis, the evaluated properties, except the flexural strength, specimen deflection, and microwear depth, were statistically compared among the subgroups separated by the aging conditions (non-aged or aged series). Moreover, the flexural strength, specimen deflection during fracture toughness testing, and microwear depth were statistically analyzed using the Kruskal–Wallis test followed by the Mann–Whitney U test with Bonferroni correction. The ratios of the broken specimens during flexural strength and modulus testing were statistically analyzed using the chi-squared test. A statistical software (IBM SPSS Statistics v28.0; IBM, Redmond, WA, USA) was used for all statistical analyses. The significance level was set at 5% ( $\alpha = 0.05$ ).

# 3. Results

## 3.1. Results of two-way ANOVA

All the  $P$  values acquired by the two-way ANOVA were less than 0.001, for the content rate of BE10 and aging in boiling water, revealing that both BE10 content and aging significantly affected the flexural modulus, fracture toughness,  $\Delta E$ , and TP.

## 3.2. Flexural strength and modulus

The results of the flexural strength and modulus evaluations are presented in **Table 3**. Regardless of the aging conditions, both flexural strength and modulus decreased with increasing BE10 contents. Within the non-aged series, the flexural strength median of BE10-0% was the highest (98.4 MPa), significantly surpassing those of BE10-50% ( $P = 0.011$ ), -60% ( $P < 0.001$ ), and -80% ( $P < 0.001$ ). However, the flexural strength median of BE10-80% was the lowest (42.1 MPa),

**Table 3.** Results of the flexural strength and modulus testing

Aging	Group	Flexural strength (MPa) <sup>#</sup>	Flexural modulus (GPa) <sup>##</sup>	Broken sepecimens (%)	Deflection at specimen break (mm) <sup>#</sup>
Non-aged	BE10-0%	98.4 [8.5] <sup>†</sup> a	3.18 ± 0.16 <sup>‡</sup> a	100.0 <sup>§</sup> a	5.49 [1.21] <sup>§§</sup>
	BE10-20%	92.6 [4.0] ab	2.75 ± 0.24 b	75.0 ab	6.92 [0.94]
	BE10-30%	89.4 [6.3] ab	2.53 ± 0.22 b	50.0 abc	7.35 [2.15]
	BE10-40%	77.9 [3.8] abc	2.14 ± 0.24 c	37.5 cbc	8.00 [0.51]
	BE10-50%	72.8 [0.8] bc	2.09 ± 0.24 c	25.0 bc	8.00 [0.28]
	BE10-60%	63.4 [3.0] c	1.75 ± 0.23 d	0.0 c	8.00 [0.00]
	BE10-80%	42.1 [2.3] c	1.27 ± 0.10 e	0.0 c	8.00 [0.00]
Aged	BE10-0%	67.5 [14.9] <sup>†</sup> A	2.98 ± 0.22 <sup>‡</sup> A	100.0 <sup>§</sup> A	3.49 [1.03]
	BE10-20%	66.6 [6.2] A	2.46 ± 0.24 B	100.0 A	4.10 [0.86]
	BE10-30%	64.7 [9.4] A	2.23 ± 0.24 B	100.0 A	5.31 [1.16]
	BE10-40%	57.9 [4.3] AB	1.74 ± 0.24 C	87.5 A	6.06 [0.92]
	BE10-50%	53.0 [1.3] ABC	1.62 ± 0.14 C	87.5 A	7.40 [0.92]
	BE10-60%	37.3 [0.9] BC	1.15 ± 0.12 D	0.0 B	8.00 [0.00]
	BE10-80%	9.3 [0.9] C	0.23 ± 0.06 E	0.0 B	8.00 [0.00]

<sup>#</sup>: Median value and interquartile range (IQR). <sup>##</sup>: Mean value and standard deviation (SD). <sup>†</sup>: Same superscripted letters indicate subgroups not statistically significantly different when compared by Kruskal-Wallis's test followed by Mann-Whitney U test with Bonferroni correction. <sup>‡</sup>: Same superscripted letters indicate subgroups not statistically significantly different when compared by 1-way ANOVA with Tukey multiple comparisons *post hoc* analysis. <sup>§</sup>: Same superscripted letters indicate subgroups not statistically significantly different when compared by the Chi-squared test with Bonferroni correction. <sup>§§</sup>: Not being statistically analyzed (just for reference). 8.00 mm of deflection indicated that the test ended before the specimen broke.

significantly lower than those of BE10-0%, -20%, and -30% ( $P < 0.001$  for all of them). Within the aged series, the flexural strength median of BE10-0% was the highest (67.5 MPa), significantly higher than those of BE10-60% ( $P = 0.001$ ) and -80% ( $P < 0.001$ ), whereas that of BE10-80% was the lowest (9.3 MPa), significantly lower than those of BE10-0% ( $P < 0.001$ ), -20% ( $P < 0.001$ ), -30% ( $P < 0.001$ ), and -40% ( $P = 0.001$ ). In contrast, within the non-aged series, the flexural modulus mean of BE10-0% was 3.18 GPa, significantly surpassing those of all the other subgroups ( $P = 0.012$  for BE10-20%;  $P < 0.001$  for BE10-30%, -40%, -50%, -60%, and -80%). However, the mean flexural modulus of BE10-80% was 1.27 GPa, significantly lower than those of all the other subgroups ( $P < 0.001$  for all of them). Within the aged series, the flexural modulus mean of BE10-0% was 2.98 GPa, significantly surpassing than those of all the other subgroups ( $P < 0.001$  for all of them), whereas that of BE10-80% was 0.23 GPa, which was significantly lower than those of all the other subgroups ( $P < 0.001$  for all of them). Regardless of the BE10 content, both flexural strength and modulus decreased with aging in boiling water.

Furthermore, the broken ratio decreased with an increase in the BE10 content, whereas the specimen deflection increased. Additionally, for the BE10-0%, -20%, -30%, -40%, and -50% specimens, aging decreased the deflection at specimen breaks, but it increased their broken ratios.

### 3.3. Fracture toughness

The results of the fracture toughness evaluation are shown in **Figure 3**. Within the non-aged series, the fracture toughness showed the highest mean value with 50% BE10 content rate (2.56 MPa·m<sup>1/2</sup>), significantly exceeding those of all the other subgroups ( $P < 0.001$  for BE10-0%, -20%, -30%, and -80%;  $P = 0.006$  and 0.007 for BE10-40% and -60%, respectively). However, the 0% BE10 specimen exhibited the lowest mean fracture toughness (1.72 MPa·m<sup>1/2</sup>), significantly

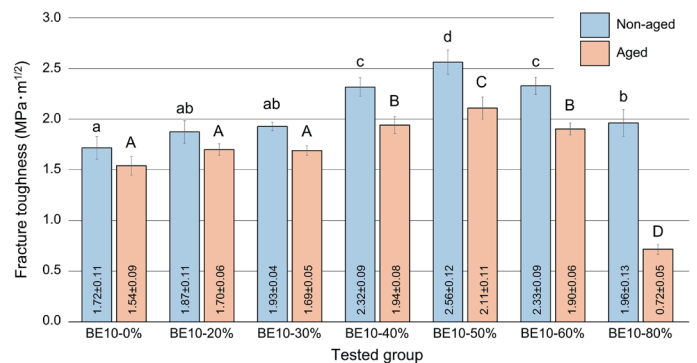


**Fig. 3.** Mean values ± standard deviations and statistical results of fracture toughness evaluation. Same superscripted letters indicate subgroups not statistically significantly different when analyzed by a one-way ANOVA with Tukey multiple comparisons *post hoc* analysis.

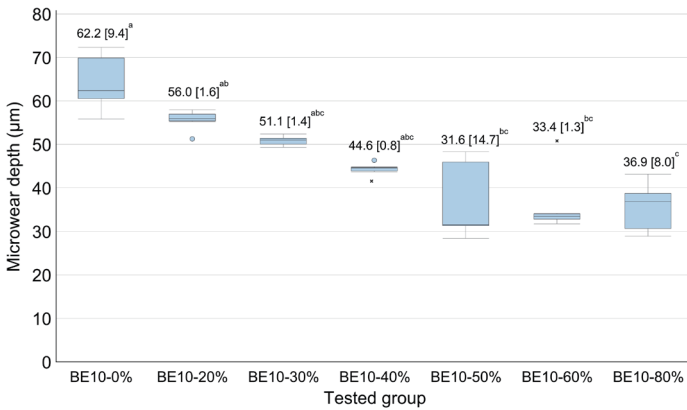
lower than those of BE10-40% ( $P < 0.001$ ), BE10-50% ( $P < 0.001$ ), BE10-60% ( $P < 0.001$ ), and BE10-80% ( $P = 0.020$ ). In contrast, within the aged series, the BE10-50% specimen exhibited the highest mean fracture toughness (2.11 MPa·m<sup>1/2</sup>), significantly higher than those of all the other subgroups ( $P < 0.001$  for BE10-0%, -20%, -30%, -60%, and -80%;  $P = 0.004$  for BE10-40%). However, BE10-80% exhibited the lowest mean fracture toughness (0.72 MPa·m<sup>1/2</sup>), significantly lower than those of all the other subgroups ( $P < 0.001$  for all of them). Regardless of the content rate of BE10, fracture toughness decreased with aging in boiling water.

The median values and interquartile ranges of the deflection at the specimen break during fracture toughness testing are listed in **Table 4**. BE10-0% exhibited the lowest deflection at specimen break, whereas BE10-80% exhibited the highest deflection. During fracture

**Table 4.** Median values and interquartile ranges of the deflection at specimen break during fracture toughness testing (mm)

Group	Non-aged series		Aged series	
BE10-0%	0.13 [0.02]	†	0.13 [0.05]	†
BE10-20%	0.19 [0.03]	a	0.17 [0.01]	a
BE10-30%	0.18 [0.00]	ab	0.16 [0.01]	a
BE10-40%	0.22 [0.01]	bc	0.20 [0.01]	bc
BE10-50%	0.27 [0.02]	cd	0.25 [0.02]	cd
BE10-60%	0.30 [0.01]	d	0.31 [0.02]	de
BE10-80%	1.26 [0.08]	d	2.45 [0.04]	e

†: Same superscripted letters indicate subgroups not statistically significantly different when compared by Kruskal-Wallis's test followed by Mann-Whitney U test with Bonferroni correction

**Fig. 4.** Median values and statistical results of microwear evaluation. Same superscripted letters indicate groups that are not statistically significantly different when compared by a Kruskal-Wallis's test followed by Mann-Whitney U test with Bonferroni correction.

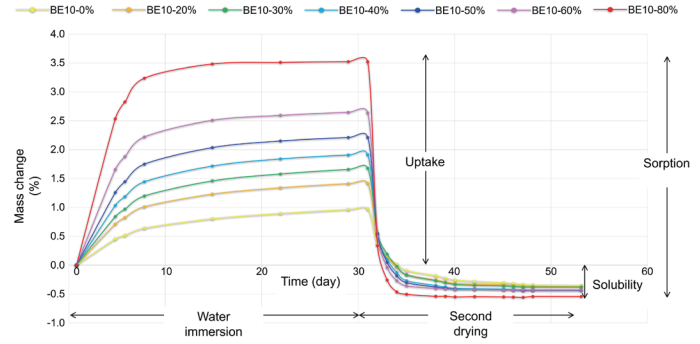
toughness testing, the specimens of all the groups other than BE10-80% were completely broken, whereas the specimens of BE10-80% were just bent.

### 3.4. Microwear resistance (microwear depth)

The microwear depth results are shown in **Figure 4**. The microwear depth median of BE10-0% was highest among all groups (62.2 µm), and it was significantly higher than those of BE10-50% ( $P = 0.007$ ), -60% ( $P = 0.014$ ), and -80% ( $P = 0.003$ ). However, the median value of the microwear depth of BE10-50% was the smallest (31.6 µm). The outlines of facets were clear in all groups except BE10-80%; BE10-80% showed an unclear outline. The cross-sectional profiles revealed that the tested groups with less than 30% BE10 contents had cup-shaped deep facets, whereas those with BE10 content exceeding 40% had flat-shaped shallow facets. Additionally, BE10-50% and -60% showed bank-shaped prominences on the facet edges.

### 3.5. Degree of double bond conversion (DC), Water sorption (WSP), and solubility (WSL)

The results of DC,  $W_{SP}$ , and  $W_{SL}$  are listed in **Table 5**. The DC,  $W_{SP}$ , and  $W_{SL}$  increased with increase the content rate of BE10. The mean DC of BE10-0% (89.5%) was significantly lower than those of all the other subgroups ( $P = 0.016$  for BE10-20%;  $P < 0.001$  for the others),

**Fig. 5.** Representative plots of mass changes (%) against time during water immersion and second drying procedure**Table 5.** Results of DC,  $W_{SP}$ , and  $W_{SL}$ 

Group	DC (%) #	$W_{SP}$ (%) #	$W_{SL}$ (%) #
BE10-0%	89.5 ± 1.1	0.96 ± 0.01	0.35 ± 0.01
BE10-20%	92.7 ± 2.0	1.40 ± 0.01	0.36 ± 0.01
BE10-30%	94.3 ± 1.6	1.66 ± 0.02	0.38 ± 0.01
BE10-40%	94.6 ± 1.7	1.89 ± 0.01	0.43 ± 0.01
BE10-50%	95.9 ± 1.1	2.20 ± 0.01	0.41 ± 0.01
BE10-60%	96.6 ± 0.6	2.61 ± 0.02	0.43 ± 0.02
BE10-80%	96.8 ± 0.9	3.48 ± 0.01	0.54 ± 0.02

#: Mean value and standard deviation (SD). †: Same superscripted letters indicate groups not statistically significantly different when compared by 1-way ANOVA with Tukey multiple comparisons post hoc analysis. DC: degree of double bond conversion;  $W_{SP}$ : water sorption;  $W_{SL}$ : water solubility.

whereas that of BE10-80% (96.8%) was the highest, significantly exceeding those of BE10-0% ( $P < 0.001$ ) and -20% ( $P = 0.002$ ). The mean  $W_{SP}$  of BE10-0% (0.96%) was significantly lower than those of all the other subgroups ( $P < 0.001$  for all of them), whereas that of BE10-80% (3.48%) was significantly higher than those of all the other subgroups ( $P < 0.001$  for all of them). Additionally, the mean  $W_{SL}$  of BE10-0% (0.35%) was the lowest, significantly lower than those of BE10-30%, -40%, -50%, -60%, and -80% ( $P = 0.008$  for BE10-30%;  $P < 0.001$  for the others), whereas that of BE10-80% (0.54%) was significantly higher than those of all the other subgroups ( $P < 0.001$  for all of them).

Representative plots of the mass changes during the  $W_{SP}$  and  $W_{SL}$  evaluations are shown in **Figure 5**. Saturation was reached 10 d after water immersion in all groups. During the second drying procedure, all groups were completely dried for 20 d.

### 3.6. Color evaluation (Spectrophotometric analysis)

Images of the specimens used for color evaluation and the results of the color evaluation are shown in **Figures 6 and 7**, respectively. The color difference between the non-aged and aged subgroups ( $\Delta E$ ) decreased with an increase in the content rate of BE10, whereas the TP increased in both the non-aged and aged series. The mean  $\Delta E$  of BE10-0% (6.00) was significantly higher than those of all the other subgroups ( $P < 0.001$  for all of them). The mean  $\Delta E$  of BE10-50%, -60%, and -80% (1.36, 1.37, and 1.45, respectively) were significantly lower than those of BE10-0%, -20%, -30%, and -40% ( $P < 0.001$  for all of them). Within the non-aged series, the mean TP of BE10-0%

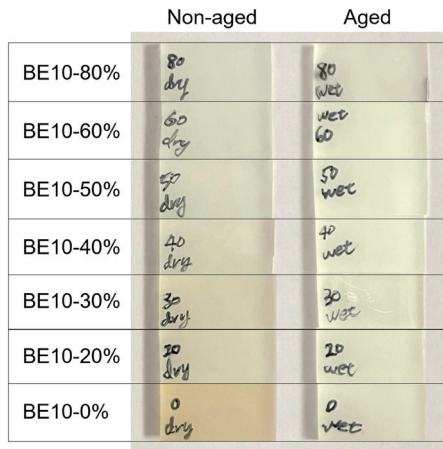


**Fig. 6.** Image of specimens for color evaluation

(49.7) was significantly lower than those of all the other subgroups ( $P < 0.001$  for all of them), whereas that of BE10-80% (52.0) was the highest, significantly higher than those of BE10-0, -20%, -30%, -40%, and -50% ( $P < 0.001$  for all of them). Within the aged series, the mean TP of BE10-0% (50.4) was the lowest, significantly lower than those of BE10-30%, -40%, -50%, -60%, and -80% ( $P = 0.001$  for BE10-30%;  $P < 0.001$  for the others), whereas that of BE10-80% (52.0) was significantly higher than those of all the other subgroups ( $P < 0.001$  for all of them). Regardless of the BE10 content rate, TP decreased with the aging in boiling water, except in the BE10-0% subgroups.

#### 4. Discussion

In this study, the effects of the content ratio of bis-EMA with different numbers of ethylene oxide units (BE3 and BE10) and aging in boiling water on several physical properties were demonstrated in experimentally fabricated additive-manufactured occlusal splint materials. The results revealed that both the BE3/BE10 content ratio and aging significantly affected all the evaluated physical properties. Furthermore, the BE10 content rate enhanced the microwear resistance, DC, and color parameters and degraded the flexural strength,

flexural modulus,  $W_{SP}$ , and  $W_{SL}$ . In addition, aging in boiling water degraded the evaluated physical properties. Therefore, both null hypotheses were rejected.

The experimental resins exhibited a higher DC with increasing BE10 contents. This result is consistent with those of previous studies[30,31]. Scranton *et al.* indicated that higher numbers of ethylene oxide units show longer spaces between unsaturates, resulting in higher monomer flexibility and enhanced monomer mobility during polymerization[32]. The polymerization of methacrylates with long and flexible chains can provide a high DC without vitrification[33]. Therefore, an increase in the number of ethylene oxide units of bis-EMA can enhance the DC of additive-manufactured PMMA-based resins for occlusal splints. The enhancement of DC can improve material biosafety[19]; however, this study did not focus on the cytotoxicity of the specimens. Further studies are required to clarify the biosafety of the additive-manufactured occlusal splints.

Despite their high DC, the subgroups with higher BE10 contents exhibited lower flexural strengths and moduli. The long chains of BE10 provided a flexible polymer that acted as a rubbery solid[30]. In this study, the lowest flexural strength and modulus, found in the BE10-80% subgroup, were still higher than those of commercial soft occlusal splint materials produced by additive manufacturing[21]. The results of this study suggest that an increase in the content of monomers with longer chains softens PMMA-based resin materials; however, monomers other than bis-EMA and UDMA should be included to achieve clinically sufficient flexibility for soft occlusal splints. In contrast, the highest flexural strength and modulus, identified in the BE10-0% subgroup, were comparable to those of the commercial materials for hard occlusal splints[22]. Flexible polymers with long chains, produced by BE10, also increased the specimen deflection during the three-point bending tests, resulting in specimen bending without any breakage.

In this study, the microwear depth decreased with increasing BE10 content, owing to the flexibility provided by the longer chains in BE. A previous study indicated that the elastic deformations on the soft occlusal splint materials can absorb shock[11]. Despite their higher microwear resistance, experimental resins with higher BE10 contents are less harmful to the antagonists, as expected for soft oc-

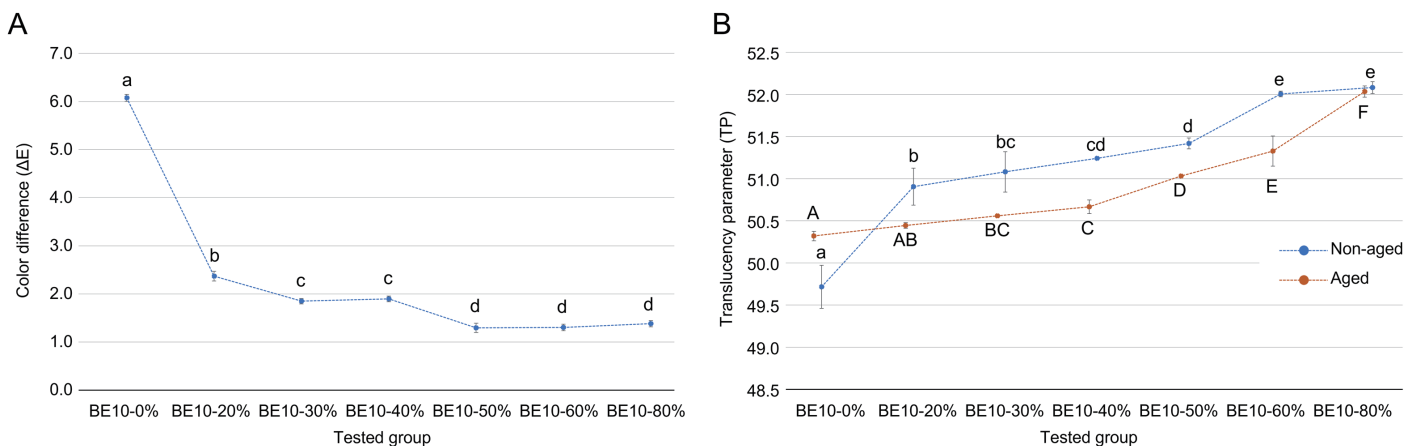


**Fig. 7.** Results of color evaluation. A: color difference between non-aged and aged subgroups ( $\Delta E$ ); and B: translucency parameter (TP). Same superscripted letters indicate subgroups that are not statistically significantly different when compared by an one-way ANOVA with Tukey multiple comparisons post hoc analysis.

clusal splints[16]. Previously, chewing forces other than 20 N, such as 5 and 50 N, were also used for wear testing of dental materials[34,35]. However, no significant difference was observed in the wear depths of the additive-manufactured resins[35]. Therefore, only one chewing force (20 N) was applied in this study.

Regarding water sorption and solubility, both  $W_{SP}$  and  $W_{SL}$  increased with increasing BE10 content. BE10-0%, -20%, and -30% subgroups revealed clinically acceptable values of  $W_{SP}$  and  $W_{SL}$  when compared to the commercial materials[21,22]. However, BE10-40%, -50%, -60%, and -80% subgroups were expected to be unsuitable for clinical use from the viewpoint of water sorption and solubility. Higher water solubility and lower DC can lead to higher cytotoxicity due to leaching of the remaining monomer[36]. Ethylene oxide units are polar functional groups (PFGs), and aromatic C–C bonds are nonpolar, indicating that an increase in the BE10 content leads to an increased number of PFGs, which promote water absorption[30]. Additionally, BE10 was more water miscible than BE3 because of the higher number of ethylene oxide units. Therefore, water can be a more efficient solvent in removing the residual monomers and oligomers in the subgroups with higher BE10 contents than in those with lower BE10 contents, resulting in the higher water solubility of the subgroups with higher BE10 contents[37]. Although the superficial layer of the inner surface of the occlusal splint is rarely removed, that of the outer surface is occasionally removed by adjusting the occlusal contact and/or surface polishing. A previous study indicated that superficial layer removal enhanced the mechanical properties, including DC and water solubility, of the PMMA-based materials used in additive-manufactured occlusal splints[38].

Unlike the other physical properties, BE10-50% subgroups in both the non-aged and aged series revealed the highest fracture toughness. The ratio of cross-linked network/long chains (i.e., aromatic groups/ethylene oxide units) might play an important role in the fracture toughness. Additionally, BE10-80% showed the largest difference between non-aged and aged subgroups (Fig. 3), suggesting that aging in boiling water can critically affect the additive-manufactured PMMA-based materials with higher BE10 contents. In this study, the fracture toughness was assessed using a single-edge notched bend (SENB) test, and the results were mainly affected by the inner structure of the specimen[39]. In contrast, the three-point bending test measured the bending properties without stress concentration. Although soft materials are not suitable for fracture tests[21], equal fracture toughness tests were performed for all groups to achieve a general understanding. These factors could explain the deviation between the results of the three-point bending and fracture toughness tests. As shown in Figure 5, BE10-80% showed the greatest water uptake, which can deteriorate the specimen inside. The largest difference between non-aged and aged subgroups was identified in BE10-80%. A previous study reported that fracture toughness of the conventional PMMA-based materials (including auto-polymerized and heat-cured materials) for occlusal splints ranges from 1.2 to 2.2 MPa·m<sup>1/2</sup>, indicating that the current fracture toughness of experimental material including bis-EMAs as photosensitive monomers is clinically sufficient, except for the aged BE10-80% subgroup.

Aging in boiling water enhances translucency. During the aging process, water molecules cleave intermolecular bonds and induce uncured monomer leakage[40,41]. Furthermore, aging in boiling water caused deterioration of the cross-linked structures and enhanced the translucency of the specimens. The color difference

between the non-aged and aged subgroups ( $\Delta E$ ) was less than 1.50 in the BE10-50%, -60%, and -80% groups. Previous studies reported the threshold value of  $\Delta E$  to be around 1.80[42,43], indicating that the color stability during aging is clinically acceptable in these three groups.

The translucency of specimens was enhanced with the increase in BE10 content, and the BE10-80% subgroups revealed the highest translucency parameter both in the non-aged and aged series. A previous study reported that experimental composites formulated with bis-EMA showed higher translucency than those formulated with Bis-GMA[44]. Bis-GMA is a structural analog of bis-EMA with secondary functional (-OH) groups that enhance cross-linked networks, indicating that a decrease in the number of cross-linked networks can enhance translucency. In this study, the number of three-dimensional chemical structures mainly depended on the two aromatic groups in bis-EMA, whereas the chain length depended on the number of ethylene oxide units. Therefore, it was concluded that BE10 enhanced the translucency of the additive-manufactured specimens with longer chain growth. Based on the results of DC%, BE10-0% had a larger amount of unpolymerized material than the other groups. The unpolymerized material can cause the specimens to be opaque and leach out during the aging procedure such that the specimens become transparent (Fig. 6). Further studies are needed to clarify the effect of unpolymerized materials on the color characteristics.

This study has some limitations. First, the aging conditions in this study were not comparable to clinical situations, although they could experimentally demonstrate degradation with hydrolytic and thermal breakdown[23,24]. Further clinical examination is needed to investigate the effect of aging under different settings such as the 5 and 55°C thermal cycle or clinical usage. Second, only two different numbers of ethylene oxide units (BE3 and BE10) were tested. There are several types of bis-EMAs with different numbers of ethylene oxide units. To clarify the detailed effect of the number of ethylene oxide units and their optimal content rate, further studies are required to test bis-EMAs with different numbers of ethylene oxide units. Finally, this study did not directly focus on the disadvantages of bis-EMAs, such as cytotoxicity, although multiple physical properties were evaluated.

## 5. Conclusions

Within the limitations of this study, it can be concluded that bis-EMA can act as a photosensitive monomer in PMMA-based occlusal splint materials for additive manufacturing. Additionally, the number of ethylene oxide units in bis-EMA and aging in boiling water impacts the physical properties of PMMA-based acrylic resins for additive-manufactured occlusal splints. Lower numbers of ethylene oxide units can enhance the flexural strength and modulus, while minimizing water sorption and solubility. In contrast, higher numbers of ethylene oxide units can enhance the microwear resistance, degree of double bond conversion, color stability during aging, and translucency. To achieve higher fracture toughness, both lower and higher numbers of ethylene oxide units are required in a specific ratio.

## Acknowledgment

This study was conducted with the support of the Biocity Turku Biomaterials Research Program ([www.biomaterials.utu.fi](http://www.biomaterials.utu.fi); accessed July 23, 2023).

## Conflict of interest statement

The authors declare no conflict of interest.

## References

- [1] Goodacre BJ, Goodacre CJ. Additive manufacturing for complete denture fabrication: a narrative review. *J Prosthodont.* 2022;31:47–51. <https://doi.org/10.1111/jopr.13426>, PMID:35313025
- [2] Ellakany P, Fouda SM, Mahrous AA, AlGhamdi MA, Aly NM. Influence of CAD/CAM milling and 3D-printing fabrication methods on the mechanical properties of 3-unit interim fixed dental prosthesis after thermo-mechanical aging process. *Polymers (Basel).* 2022;14:4103. <https://doi.org/10.3390/polym14194103>, PMID:36236050
- [3] Al Hamad KQ, Al-Rashdan BA, Ayyad JQ, Al Omrani LM, Sharoh AM, Al Nimri AM, et al. Additive manufacturing of dental ceramics: a systematic review and meta-analysis. *J Prosthodont.* 2022;31:e67–86. <https://doi.org/10.1111/jopr.13553>, PMID:35675133
- [4] Dao TT, Lavigne GJ. Oral splints: the crutches for temporomandibular disorders and bruxism? *Crit Rev Oral Biol Med.* 1998;9:345–61. <https://doi.org/10.1177/10454411980090030701>, PMID:9715371
- [5] Klasser GD, Greene CS. Oral appliances in the management of temporomandibular disorders. *Oral Surg Oral Med Oral Pathol Oral Radiol Endod.* 2009;107:212–23. <https://doi.org/10.1016/j.tripleo.2008.10.007>, PMID:19138639
- [6] Friction J, Look JO, Wright E, Alencar FG Jr, Chen H, Lang M, et al. Systematic review and meta-analysis of randomized controlled trials evaluating intraoral orthopedic appliances for temporomandibular disorders. *J Orofac Pain.* 2010;24:237–54. <https://europepmc.org/article/MED/20664825>, PMID:20664825
- [7] Carlsson GE, Johansson A, Lundqvist S. Occlusal wear: A follow-up study of 18 subjects with extensively worn dentitions. *Acta Odontol Scand.* 1985;43:83–90. <https://doi.org/10.3109/00016358509046491>, PMID:3863449
- [8] Lobbezoo F, Van Der ZAAG J, Van SELMS MKA, Hamburger HL, Naeije M. Principles for the management of bruxism. *J Oral Rehabil.* 2008;35:509–23. <https://doi.org/10.1111/j.1365-2842.2008.01853.x>, PMID:18557917
- [9] Kathariya R, Devanoorkar A, Golani R, Shetty N, Vallakata V, Bhat MY. To splint or not to splint: the current status of periodontal splinting. *J Int Acad Periodontol.* 2016;18:45–56. <https://europepmc.org/article/MED/27128157>, PMID:27128157
- [10] Uchida H, Wada J, Watanabe C, Nagayama T, Mizutani K, Mikami R, et al. Effect of night dentures on tooth mobility in denture wearers with sleep bruxism: A pilot randomized controlled trial. *J Prosthodont Res.* 2021;66:564–71. [https://doi.org/10.2186/jpr.JPR\\_D\\_21\\_00230](https://doi.org/10.2186/jpr.JPR_D_21_00230), PMID:34789636
- [11] Wada J, Wada K, Garoushi S, Shinya A, Wakabayashi N, Iwamoto T, et al. Effect of 3D printing system and post-curing atmosphere on micro- and nano-wear of additive-manufactured occlusal splint materials. *J Mech Behav Biomed Mater.* 2023;142:105799. <https://doi.org/10.1016/j.jmbbm.2023.105799>, PMID:37028121
- [12] Okeson JP. The effects of hard and soft occlusal splints on nocturnal bruxism. *J Am Dent Assoc.* 1987;114:788–91. <https://doi.org/10.14219/jada.archive.1987.0165>, PMID:3475357
- [13] Quayle AA, Gray RJM, Metcalfe RJ, Guthriet E, Wastell D. Soft occlusal splint therapy in the treatment of migraine and other headaches. *J Dent.* 1990;18:123–9. [https://doi.org/10.1016/0300-5712\(90\)90048-J](https://doi.org/10.1016/0300-5712(90)90048-J), PMID:2401762
- [14] Cruz-Reyes RA, Martínez-Aragón I, Guerrero-Arias RE, García-Zura DA, González-Sánchez LE. Influence of occlusal stabilization splints and soft occlusal splints on the electromyographic pattern, in basal state and at the end of six weeks treatment in patients with bruxism. *Acta Odontol Latinoam.* 2011;24:66–74. <https://europepmc.org/article/MED/22010409>, PMID:22010409
- [15] Silva CAGD, Grossi ML, Araldi JC, Corso LL. Can hard and/or soft occlusal splints reduce the bite force transmitted to the teeth and temporomandibular joint discs? A finite element method analysis. *Cranio.* 2023;41:298–305. <https://doi.org/10.1080/08869634.2020.1853464>, PMID:33280545
- [16] Ramfjord SP, Ash MM. Reflections on the Michigan occlusal splint. *J Oral Rehabil.* 1994;21:491–500. <https://doi.org/10.1111/j.1365-2842.1994.tb01164.x>, PMID:7996334
- [17] Gujjari AK, Sriharsha P, Dhakshaini MR, Prashant A. Comparative evaluation of salivary cortisol levels in bruxism patients before and after using soft occlusal splint: an in vivo study. *Contemp Clin Dent.* 2018;9:182–7. [https://doi.org/10.4103/ccd.ccd\\_756\\_17](https://doi.org/10.4103/ccd.ccd_756_17), PMID:29875558
- [18] Szczesio-Wlodarczyk A, Domarecka M, Kopacz K, Sokolowski J, Bociong K. An evaluation of the properties of urethane dimethacrylate-based dental resins. *Materials (Basel).* 2021;14:2727. <https://doi.org/10.3390/ma14112727>, PMID:34064213
- [19] Lin CH, Lin YM, Lai YL, Lee SY. Mechanical properties, accuracy, and cytotoxicity of UV-polymerized 3D printing resins composed of Bis-EMA, UDMA, and TEGDMA. *J Prosthet Dent.* 2020;123:349–54. <https://doi.org/10.1016/j.prosdent.2019.05.002>, PMID:31202550
- [20] Gibreel M, Perea-Lowery L, Vallittu PK, Lassila L. Characterization of occlusal splint materials: CAD-CAM versus conventional resins. *J Mech Behav Biomed Mater.* 2021;124:104813. <https://doi.org/10.1016/j.jmbbm.2021.104813>, PMID:34530298
- [21] Wada J, Wada K, Gibreel M, Wakabayashi N, Iwamoto T, Vallittu P, et al. Effect of 3D printer type and use of protection gas during post-curing on some physical properties of soft occlusal splint material. *Polymers (Basel).* 2022;14:4618. <https://doi.org/10.3390/polym14214618>, PMID:36365611
- [22] Wada J, Wada K, Gibreel M, Wakabayashi N, Iwamoto T, Vallittu PK, et al. Effect of nitrogen gas post-curing and printer type on the mechanical properties of 3D-printed hard occlusal splint material. *Polymers (Basel).* 2022;14:3971. <https://doi.org/10.3390/polym14193971>, PMID:36235919
- [23] Ozcan M, Barbosa S, Melo R, Galhano G, Bottino M. Effect of surface conditioning methods on the microtensile bond strength of resin composite to composite after aging conditions. *Dent Mater.* 2007;23:1276–82. <https://doi.org/10.1016/j.dental.2006.11.007>, PMID:17174388
- [24] Oja J, Lassila L, Vallittu PK, Garoushi S. Effect of accelerated aging on some mechanical properties and wear of different commercial dental resin composites. *Materials (Basel).* 2021;14:2769. <https://doi.org/10.3390/ma14112769>, PMID:34071137
- [25] ISO 20795-1: 2013. Base polymers-part 1: Denture base polymers.
- [26] Garoushi S, Lassila L, Vallittu PK. Impact of fast high-intensity versus conventional light-curing protocol on selected properties of dental composites. *Materials (Basel).* 2021;14:1381. <https://doi.org/10.3390/ma14061381>, PMID:33809096
- [27] Gibreel M, Perea-Lowery L, Vallittu PK, Garoushi S, Lassila L. Two-body wear and surface hardness of occlusal splint materials. *Dent Mater J.* 2022;41:916–22. <https://doi.org/10.4012/dmj.2022-100>, PMID:36288940
- [28] Viljanen EK, Skrifvars M, Vallittu PK. Dendrimer/methyl methacrylate co-polymers: residual methyl methacrylate and degree of conversion. *J Biomater Sci Polym Ed.* 2005;16:1219–31. <https://doi.org/10.1163/156856205774269566>, PMID:16268249
- [29] ISO/CIE. ISO/CIE 11664-4. Colorimetry-part. 2019;4:CIE1976L. \*a\*b\*colour space.
- [30] Ogliafi F, Ely C, Zanchi C, Fortes C, Samuel S, Demarco F, et al. Influence of chain extender length of aromatic dimethacrylates on polymer network development. *Dent Mater.* 2008;24:165–71. <https://doi.org/10.1016/j.dental.2007.03.007>, PMID:17531312
- [31] Fonseca ASQS, Labruna Moreira AD, de Albuquerque PPAC, de Menezes LR, Pfeifer CS, Schneider LFJ. Effect of monomer type on the C C degree of conversion, water sorption and solubility, and color stability of model dental composites. *Dent Mater.* 2017;33:394–401. <https://doi.org/10.1016/j.dental.2017.01.010>, PMID:28245929
- [32] Scranton AB, Bowman CN, Klier J, Peppas NA. Polymerization reaction dynamics of ethylene glycol methacrylates and dimethacrylates by calorimetry. *Polymer (Guildf).* 1992;33:1683–9. [https://doi.org/10.1016/0032-3861\(92\)91067-C](https://doi.org/10.1016/0032-3861(92)91067-C)
- [33] Anseth KS, Kline LM, Walker TA, Anderson KJ, Bowman CN. Reaction kinetics and volume relaxation during polymerizations of multiethylene glycol dimethacrylates. *Macromolecules.* 1995;28:2491–9. <https://doi.org/10.1021/ma00111a050>

- [34] Huettig F, Kustermann A, Kuscü E, Geis-Gerstorfer J, Spintzyk S. Polishability and wear resistance of splint material for oral appliances produced with conventional, subtractive, and additive manufacturing. *J Mech Behav Biomed Mater.* 2017;75:175–9. <https://doi.org/10.1016/j.jmbbm.2017.07.019>, PMID:28734259
- [35] Wesemann C, Spies BC, Sterzenbach G, Beuer F, Kohal R, Wemken G, et al. Polymers for conventional, subtractive, and additive manufacturing of occlusal devices differ in hardness and flexural properties but not in wear resistance. *Dent Mater.* 2021;37:432–42. <https://doi.org/10.1016/j.dental.2020.11.020>, PMID:33288324
- [36] Aati S, Akram Z, Shrestha B, Patel J, Shih B, Shearston K, et al. Effect of post-curing light exposure time on the physico-mechanical properties and cytotoxicity of 3D-printed denture base material. *Dent Mater.* 2022;38:57–67. <https://doi.org/10.1016/j.dental.2021.10.011>, PMID:34815094
- [37] Hansen CM. Hansen solubility parameters - a user's handbook. 2nd ed. Boca Raton; CRC Press; 2007. Chapter 1.
- [38] Wada J, Wada K, Gibreel M, Wakabayashi N, Iwamoto T, Vallittu P, et al. Effect of surface polishing on physical properties of an occlusal splint material for additive manufacturing under protection gas post-curing condition. *Polymers (Basel).* 2023;15:625. <https://doi.org/10.3390/polym15030625>, PMID:36771926
- [39] Bechtle S, Fett T, Rizzi G, Habelitz S, Schneider GA. Mixed-mode stress intensity factors for kink cracks with finite kink length loaded in tension and bending: application to dentin and enamel. *J Mech Behav Biomed Mater.* 2010;3:303–12. <https://doi.org/10.1016/j.jmbbm.2009.12.004>, PMID:20346898
- [40] Göpferich A. Mechanisms of polymer degradation and erosion. *Biomaterials.* 1996;17:103–14. [https://doi.org/10.1016/0142-9612\(96\)85755-3](https://doi.org/10.1016/0142-9612(96)85755-3), PMID:8624387
- [41] Ferracane JL, Berge HX, Condon JR. In vitro aging of dental composites in water? Effect of degree of conversion, filler volume, and filler/matrix coupling. *J Biomed Mater Res.* 1998;42:465–72. [https://doi.org/10.1002/\(SICI\)1097-4636\(19981205\)42:3<465::AID-JBM17>3.0.CO;2-F](https://doi.org/10.1002/(SICI)1097-4636(19981205)42:3<465::AID-JBM17>3.0.CO;2-F), PMID:9788511
- [42] Paravina RD, Ghinea R, Herrera LJ, Bona AD, Igiel C, Linninger M, et al. Color difference thresholds in dentistry. *J Esthet Restor Dent.* 2015;27(suppl 1):S1–9. <https://doi.org/10.1111/jerd.12149>, PMID:25886208
- [43] Thoma D, Ioannidis A, Fehmer V, Michelotti G, Jung R, Sailer I. Threshold values for the perception of color changes in human teeth. *Int J Periodontics Restorative Dent.* 2016;36:777–83. <https://doi.org/10.11607/prd.2937>, PMID:27922642
- [44] Leyva del Rio D, Johnston WM. Optical characteristics of experimental dental composite resin materials. *J Dent.* 2022;118:103949. <https://doi.org/10.1016/j.jdent.2022.103949>, PMID:35026354



This is an open-access article distributed under the terms of Creative Commons Attribution-NonCommercial License 4.0 (CC BY-NC 4.0), which allows users to distribute and copy the material in any format as long as credit is given to the Japan Prosthodontic Society. It should be noted however, that the material cannot be used for commercial purposes.